Ventral Tegmental Area Neurotensin Signaling Links the Lateral Hypothalamus to Locomotor Activity and Striatal Dopamine Efflux in Male Mice

Christa M. Patterson,* Jenny-Marie T. Wong,* Gina M. Leinninger, Margaret B. Allison, Omar S. Mabrouk, Chelsea L. Kasper, Ian E. Gonzalez, Alexander Mackenzie, Justin C. Jones, Robert T. Kennedy, and Martin G. Myers, Jr.

Division of Metabolism, Endocrinology and Diabetes (C.M.P., G.M.L., C.L.K., I.E.G., A.M., J.C.J., M.G.M.), Department of Internal Medicine and Departments of Chemistry (J.-M.T.W., O.S.M., R.T.K.) and Molecular and Integrative Physiology (M.B.A., M.G.M.), University of Michigan, Ann Arbor, Michigan 48109-1055

Projections from the lateral hypothalamic area (LHA) innervate components of the mesolimbic dopamine (MLDA) system, including the ventral tegmental area (VTA) and nucleus accumbens (NAc), to modulate motivation appropriately for physiologic state. Neurotensin (NT)-containing LHA neurons respond to multiple homeostatic challenges and project to the VTA, suggesting that these neurons could link such signals to MLDA function. Indeed, we found that pharmacogenetic activation of LHA NT neurons promoted prolonged DA-dependent locomotor activity and NAc DA efflux, suggesting the importance of VTA neurotransmitter release by LHA NT neurons for the control of MLDA function. Using a microdialysis-mass spectrometry technique that we developed to detect endogenous NT in extracellular fluid in the mouse brain, we found that activation of LHA NT cells acutely increased the extracellular concentration of NT (a known activator of VTA DA cells) in the VTA. In contrast to the prolonged elevation of extracellular NAc DA, however, VTA NT concentrations rapidly returned to baseline. Intra-VTA infusion of NT receptor antagonist abrogated the ability of LHA NT cells to increase extracellular DA in the NAc, demonstrating that VTA NT promotes NAc DA release. Thus, transient LHA-derived NT release in the VTA couples LHA signaling to prolonged changes in DA efflux and MLDA function. **(*Endocrinology* 156: 1692–1700, 2015)**

Dopamine (DA)-containing neurons of the ventral tegmental area (VTA) project widely in the forebrain, including to the nucleus accumbens (NAc); the release of DA within the NAc mediates motivation and is required for volitional activity (1). Indeed, artificial activation of the VTA→NAc mesolimbic DA (MLDA) circuit underlies the motivating properties of natural rewards and drugs of abuse. Under normal conditions, a variety of physiologic and environmental parameters modulate NAc DA release to control motivation appropriately for conditions. Many physiologic parameters (including those related to fluid balance, energy stores, endocrine status, and infection) are initially sensed in the hypothalamus (2), which integrates these inputs and relays a composite signal to the MLDA and other effector systems.

The lateral hypothalamic area (LHA) represents the major link between the hypothalamus and the MLDA system. Indeed, animals will self-administer electrical or optogenetic stimulation of lateral hypothalamic neurons (intrahypothalamic self-stimulation), consistent with the

ISSN Print 0013-7227 ISSN Online 1945-7170
Printed in U.S.A.

Received December 10, 2014. Accepted February 24, 2015.
First Published Online March 3, 2015

* C.M.P. and J.-M.T.W. contributed equally to this work.

Abbreviations: AA, amino acid; AAV, adenovirus-associated virus; AP, anterior-posterior; cFos, product of the Fos gene; CNO, clozapine-N-oxide; DA, dopamine; D1R, dopamine receptor-1; DREADD, designer receptors exclusively activated by designer drug; dsRed, red fluorescent protein; DV, dorsal-ventral; GABA, gamma amino butyric acid; HA, hemaglutinin; HCRT, hypocretin; IR, immunoreactivity; LC-MS, liquid chromatography-mass spectrography; LepRb, leptin receptor; LHA, lateral hypothalamic area; ML, medial-lateral; MLDA, mesolimbic DA; NAc, nucleus accumbens; NT, neurotensin; NTR1, NT receptor 1; VCO_2, carbon dioxide production; VO_2, oxygen consumption; VTA, ventral tegmental area.

motivating properties of LHA output (3, 4). Specific subsets of LHA neurons likely mediate distinct aspects of MLDA regulation. LHA neurons that contain the neuropeptide hypocretin (HCRT) (also known as orexin) project to the VTA and promote MLDA activity (5, 6). Melanin-concentrating hormone-containing LHA neurons project to the NAc (among other places) and modulate motivated behaviors such as feeding (7).

The peptide neurotensin (NT) has been implicated in control of feeding and the MLDA system. A substantial percentage of VTA DA neurons express NT receptor 1 (NTR1), administration of NT in rodents activates VTA DA neurons and stimulates DA release in the NAc, and NT injection acutely decreases feeding and alters locomotor activity (8–12). NT neurons are found throughout the brain, including the LHA. LHA NT neurons innervate and inhibit local LHA HCRT neurons, as well as projecting directly to the VTA (4, 13, 14). Many LHA NT neurons express the leptin receptor (LepRb) and thus respond directly to leptin (an adipokine that signals the repletion of body energy stores); ablation of LepRb from LHA NT neurons prevents the inhibition of HCRT neurons by leptin and blunts MLDA function and locomotor activity (13). Furthermore, many VTA DA neurons contain NTR1 and NT can augment the activity of VTA DA neurons (by enhancing the postsynaptic response to Glu on N-methyl-D-aspartate receptors) (8). Similarly, intrahypothalamic self-stimulation for optogenetic activation of LHA neurons is blunted by NTR1 antagonists (4). Thus, LHA NT neurons, by releasing NT into the VTA, could modulate MLDA function to link hypothalamic signals to NAc DA release. Here, we interrogate this putative circuit by pharmacogenetically activating LHA NT neurons to examine VTA and NAc neurotransmitter release, along with resultant locomotor behavior.

Materials and Methods

Animals

Adult mice (8–12 wk of age) were used for all experiments. All animals were bred in our colony in the Unit for Laboratory Animal Medicine at the University of Michigan in accordance with the guidelines and approval of the University Committee on the Care and Use of Animals. Mice were housed in a temperature and humidity controlled room with 12-hour light, 12-hour dark cycles with access to food and water ad libitum. Adequate measures were taken to prevent animal pain and discomfort throughout the course of the experiments. In addition, all animal experiments were conducted within the guidelines of Animal Research Reporting in vivo Experiments. The Nt^{cre}, $Rpl22^{tm1.1Psam}$ (Rpl22-HA reporter), $Gt(ROSA)26^{Sortm14(CAG-tdTomato)Hze}$ (ROSA26-tdTomato), and *GAD1-GFP* mouse lines have been previously described (13, 15, 16). The Nt^{cre} and $Rpl22^{tm1.1Psam}$ or $Gt(ROSA)26^{Sortm14(CAG-tdTomato)Hze}$ mice were intercrossed to generate compound heterozygous reporter mice (Nt^{cre}-HA and Nt^{cre}-tdTomato, respectively).

Stereotaxic injection and VTA cannulation

Nt^{cre} mice were anesthetized via isoflurane before the initiation of surgical procedures. Stereotaxic viral injections were made bilaterally into the LHA with a guide cannula and injector using the next coordinates: anterior-posterior −1.34, medial-lateral ±1.13, dorsal-ventral −5.2. 300 nL of adenovirus-associated virus (AAV)-hM3Dq-mCherry (17, 18) (prepared by the University of Iowa or University of North Carolina Vector Core) was injected into the LHA using a 500-nL Hamilton syringe at the rate of 20 nL/min. Bilateral injections were performed in animals receiving AAV-hM3Dq to ensure adequate infection. After 5 minutes of time after injection, the injector and cannula were removed from the animal and the incision site was closed. Mice were allowed 1–2 weeks to recover before experimentation.

For experiments requiring intra-VTA injection of the water soluble NT1R antagonist, SR142948A (Sigma), mice were implanted with an indwelling 26-guage stainless steel cannula with a removable dummy injector (Plastics One) aimed at the VTA using the next coordinates: AP −3.2, ML −0.5, DV −4.3. After 1 week of recovery, the dummy was removed and replaced with an injector with a 4.4-mm projection used to deliver 65 nL of SR142948A (5μM), 15 minutes before ip clozapine-N-oxide (CNO) administration.

Metabolic and behavioral profiling

Nt^{cre};LHA-hM3Dq-mCherry mice (n = 5) were analyzed via the Comprehensive Laboratory Monitoring System (Columbus Instruments), as previously described (13). Briefly, mice were placed into the sealed chambers with ad libitum access to food and water. After 2 days of acclimation, animals were treated with vehicle for 2 days and then with CNO (0.3 mg/kg, IP) for 2 days; treatments were every 12 hours (6 AM and 6 PM). Oxygen consumption (VO_2), carbon dioxide production (VCO_2), spontaneous motor activity, and Z-activity were monitored continuously during this time. Data shown are for the first 12 hours after each treatment.

Open-field activity was determined in separate cohorts of Nt^{cre};LHA-hM3Dq-mCherry mice (n = 6–8). Mice were removed from their home cages during the light-cycle and acclimated for 2 hours in an open-field arena (ENV-017M; Med Associates, Inc) in the absence of food and water. After acclimation, open-field activity was recorded every minute after 30 minutes of baseline, 30 minutes after saline injection, 30 minutes after antagonist injection (when applicable), and 90 minutes after CNO. For experiments involving dopamine receptor 1 (D1R) antagonism, mice were pretreated with the D1R antagonist, SCH23390 (0.1 mg/kg, ip, dissolved in PBS; Sigma), 30 minutes after vehicle administration and 30 minutes before CNO treatment.

Mouse locomotor behavior during microdialysis (n = 6) was monitored using Logitech webcams above a Raturn (Bioanalytical Systems, Inc) as previously described (19, 20). Webcams used a custom motion-monitoring program (Mark Dow) through image acquisition toolbox in Matlab 2009 (Mathworks, Natick) software. Threshold of motion detection software was selected to not detect small motions (such as breathing or whisker movement) but only large motions such as walking, running, and

Table 1. Antibody Table

Peptide/Protein Target	Antigen Sequence (if known)	Name of Antibody	Manufacturer, Catalog Number, and/or Name of Individual Providing the Antibody	Species Raised in; Monoclonal or Polyclonal	Dilution Used
cFos		Anti-cFOS	Santa Cruz Biotechnology, Inc	Goat	1:1000
dsRed		Anti-dsRed	Clontech	Rabbit	1:1000

rearing. Data were collected every 1 minute and then binned into longer intervals to correlate to facilitate comparisons with data from neurochemical assays.

Perfusion fixation and immunohistochemistry

After experimentation, all mice were perfused with fixative to verify viral, indwelling cannula, and/or microdialysis probe placement. Mice were only included in the results if mCherry expressing cell bodies were confined to the LHA, and histological analysis revealed correct cannula placement.

Animals received an overdose of sodium pentobarbital and were then perfused transcardially with PBS (pH 7.4) followed by 10% formalin. The brain was removed and postfixed in 10% formalin for 2–4 hours and then dehydrated in 30% sucrose in PBS until the time of sectioning. Brains were cut on a freezing sliding microtome in 30-μm coronal sections on a sliding microtome, collected in 4 representative series, and stored at −20°C in cryoprotectant. Sections were thoroughly washed with PBS to remove the cryoprotectant before immunostaining.

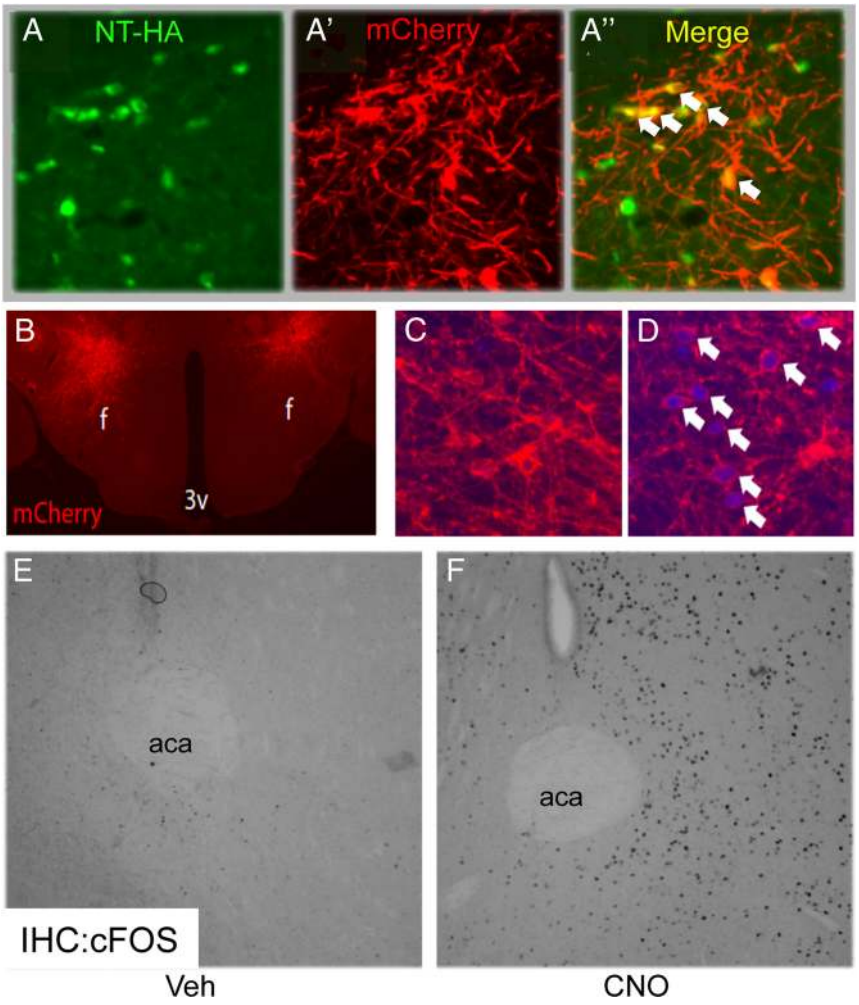

Figure 1. Activation of LHA NT neurons increases cFOS in LHA NT cells and in the NAc. Cre-inducible AAV-hM3Dq-mCherry was injected unilaterally into the LHA of male Nt^{cre} HA (A, A′, and A″) or bilaterally into the LHA of Nt^{cre} mice (B–F). A, A′, and A″, Representative image showing NT-HA-IR (A), mCherry-IR (A′), and merged channels (A″) in the LHA. Arrows denote representative colocalized cells. B, Representative image of mCherry-IR in the hypothalamus after bilateral injection. C and D, Animals were injected with vehicle (Veh; ip) (C) or CNO (0.3 mg/kg, ip) (D) and perfused 2 hours later. Shown are representative images of mCherry-IR (red) and cFOS-IR (purple, pseudocolored). Arrows denote colocalized neurons. F, fornix; 3v, third cerebral ventricle. E and F, Representative images showing cFOS-IR (black) after Veh (E) or CNO (F) in the NAc. aca, anterior commissure.

To immunostain for the product of the *Fos* gene (cFos), free-floating brain sections were pretreated consecutively with the next reagents in PBS: 1% H_2O_2, 0.3% glycine, and 0.03% sodium dodecyl sulfate. Samples were then blocked in 3% normal donkey serum/3% Triton X-100 in PBS and then incubated with goat anti-cFos (1:1000; Santa Cruz Biotechnology, Inc) overnight in the same buffer. Sections were washed in PBS, incubated in biotinylated donkey-antigoat (1:200; Jackson ImmunoResearch) for 2 hours, followed by avidin-biotin-complex labeling (Vectastain Elite kit; Vector Laboratories). Signals were developed with metal-enhanced diaminobenzidine (Thermo-Pierce) resulting in a brown precipitate.

For mCherry/tdTomato and hemaglutinin (HA) immunostaining, sections were blocked as described above and then incubated in rabbit anti-red fluorescent protein (dsRed) (1:1000; Clontech) or mouse anti-HA (1:1000; Covance) overnight, respectively. Brain sections were washed and then incubated with Alexa Fluor-conjugated secondary antibodies (1:200; Invitrogen). Sections were mounted onto gelatin-coated slides and coverslipped with ProLong Antifade mounting medium (Life Technologies) (for antibodies, see Table 1).

Microscopy and image analysis

Microscopic images were obtained using an Olympus BX-51 microscope with a DP30BW camera (Olympus). Images from fluorescent labeling experiments were pseudocolored and merged using Adobe Photoshop.

Microdialysis, analysis of amino acid (AA), and neuropeptide concentrations

Custom-made side-by-side microdialysis probes (1-mm dialyzing membrane) were inserted into NAc or VTA using the next coordinates: AP +1.30, ML ±1.20, DV −4.85; and AP −2.98, ML ±0.48, DV −5.17, respectively. For the monoamine and AA assay, probes were made using regenerated cellulose (Spectrum Laboratories) and inserted bilaterally in the NAc. For neuropeptide measurement in the VTA, probes were made using AN69 membrane (Hospal) and a single probe was inserted. For NT antagonist experiments, a dialysis probe was implanted in the NAc and a microinjection cannula (Plastics One) was implanted in the ipsilateral VTA. Probes and cannulae were secured with skull screws and acrylic dental cement. After surgery, mice were allowed to recover for 24 hours with free access to food and water.

Experiments were performed 24 hours after probe implantation. Microdialysis probes were flushed at a flow rate of 2 μL/min with artificial cerebrospinal fluid for 30 minutes using a Fusion 400 syringe pump (Chemyx). Perfusion flow rate was then reduced to 1 μL/min for monoamine and AA assay or 0.6 μL/min for the NT assay and allowed to flush for an additional 1.5 hours before baseline collections.

Samples were collected every 5 minutes for monoamine and AA assay in the NAc and every 20 minutes for the monoamine and AA and NT assays in the VTA. The total volume of dialysate for VTA NT was 12 μL, of which 3 μL were removed, and 1 μL acetonitrile was added for analysis by the monoamine and AA assay described below.

Monoamine and AA analysis

Samples were analyzed according to a slightly modified version of a recently described method (21). To 5-μL samples, we added 2.5 μL of 100mM sodium tetraborate, 2.5 μL of benzoyl chloride (2% in acetonitrile vol/vol), 2.5 μL of internal standard, and 2.5-μL d4-acetylcholine internal standard before liquid chromatography-mass spectrography (LC-MS) analysis. For VTA, 3-μL samples 1.5 μL of each reagent listed above were added before LC-MS analysis. Samples were analyzed using a Waters nanoAquity UPLC equipped with an Acquity HSS T3 C18 column (1 × 100 mm, 1.8 μm, 100-Å pore size) interfaced to an Agilent 6410 triple quadrupole mass spectrometer. Mobile phase A consisted of 10mM ammonium formate and 0.15% (vol/vol) formic acid in water. Mobile phase B was acetonitrile. The flow rate was 100 μL/min, and sample injection volume was 5 μL. The mobile phase gradient was: initial, 0% B; 0.01 minutes, 23% B; 2.51 minutes, 23% B; 3 minutes, 50% B; 5.2 minutes, 60% B; 6.46 minutes, 65%; 6.47 minutes, 100% B; 7 minutes, 100% B; 7.01 minutes, 0% B; and 8.0 minutes, 0% B. Peaks were processed using Agilent MassHunter Workstation Quantitative Analysis for QQQ version B.05.00.

NT detection with capillary LC-MS

NT was measured using a capillary LC-MS method similar to that previously described (19, 22). Capillary columns and electrospray ionization emitter tips were made in-house (19). Five-microliter samples were injected using a WPS-3000TPL autosampler, desalted by rinsing the column with 0.1% formic acid in water at 3500 psi for 8 minutes using a 100DM high pressure syringe pump (Teledyne ISCO), and then separated by a gradient elution with an Agilent 1100 HPLC pump. For the gradient, mobile phase A was 0.1% formic acid in H_2O and mobile phase B was 0.1% formic acid in MeOH. The mobile phase gradient was as follows: initial, 10% B; 2 minutes, 100% B; 6 minutes, 100% B; 6.1 minute, 10% B; and 8 minutes, 10% B. A Valco 6-port valve was used to switch between loading/desalting and elution. Assays were controlled automatically using Thermo-Fisher Xcalibur software.

The column was interfaced to a PV-550 nanospray electrospray ionization source (New Objective) coupled to a Thermo-Fischer LTQ XL linear ion trap mass spectrometer. The MS^2 pathway for NT (doubly charged) was m/z 558.7 → m/z 579.0 with an isolation width set at 3 m/z. Standard addition tests with NT showed that there was no significant effect of artificial cerebrospinal fluid matrix. In vitro recovery of NT was 14 ± 1%.

Statistics

Student's *t* test was used when only 2 groups were compared. One-way ANOVA with Bonferroni post hoc analysis was used when comparing 3 or more groups.

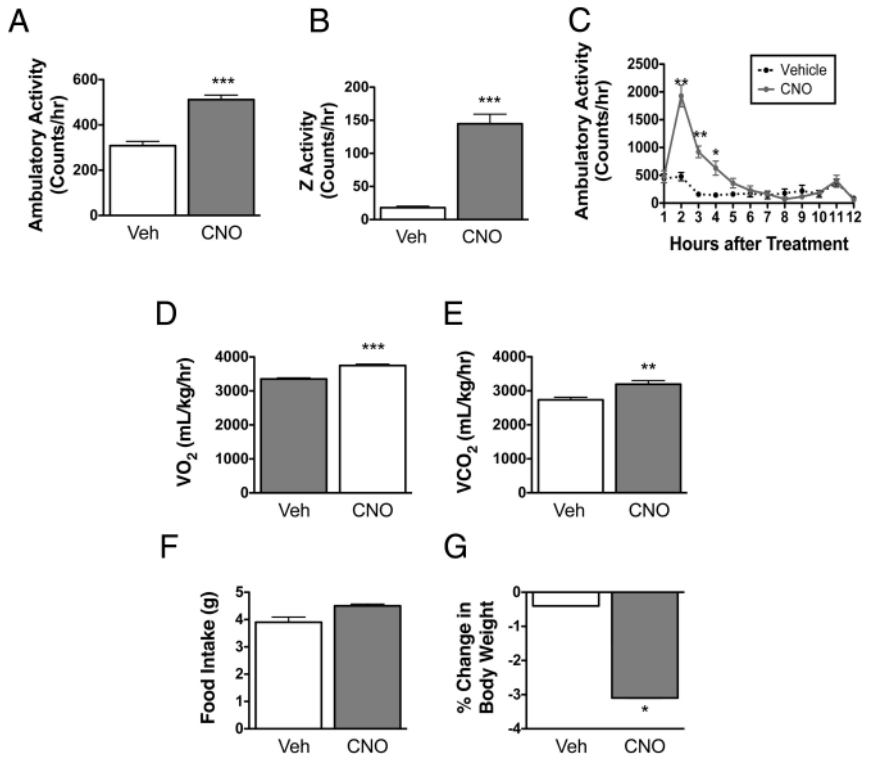

Figure 2. Activation of LHA NT neurons increases ambulatory activity and energy expenditure. *Nt*^{cre};LHA-hM3Dq-mCherry mice were acclimated to the Comprehensive Laboratory Monitoring System (CLAMS) for 2 days and treated with vehicle (Veh; ip) or CNO (0.3 mg/kg, ip) on separate days. Ambulatory activity (A and C), Z-activity (B), VO_2 (D) and VCO_2 (E) (both corrected for lean body mass), food intake (F), and change in body weight (G) are plotted for the subsequent 12 hours. All data are plotted at mean ± SEM, n = 8. Significance was determined by Student's *t* test. *, $P < .05$; **, $P < .01$; ***, $P \leq .001$.

Data were analyzed and graphs were generated using GraphPad Prism software. Differences were deemed significant if $P < .05$. Activity data are binned and presented as mean ± SEM. All in vivo microdialysis data are expressed as percent baseline ± SEM.

Results

Activation of LHA NT neurons promotes DA-dependent activity

LHA NT neurons respond to a variety of physiologic signals (including nutritional cues, dehydration, and inflammation), and are hypothesized to play a role in the modulation of motivated behaviors, including locomotor activity, in response to these signals (13, 23, 24). To understand the function of LHA NT cells and the neural mechanisms by which they mediate their effects, we employed the stereotaxic injection of AAVs that mediate the cre-dependent expression of designer receptors exclusively activated by designer drugs (DREADDs) (expressed as DREADD-mCherry fusion proteins) (17, 18). DREADDs are genetically engineered muscarinic receptor variants that are insensitive to endogenous ligands, but which are activated by the otherwise biologically inert CNO (17, 18); CNO activates neurons containing the G_q-coupled $hM3D_q$ DREADD variant. To confirm the cre-dependent expression of hM3Dq-mCherry in LHA NT neurons after viral injection, we performed unilateral injections of AAV-$hM3D_q$-mCherry into the LHA of Nt^{cre}-HA mice, which express an HA epitope-tagged ribosomal protein (16). Immunostaining against HA and mCherry demonstrated the restriction of hMD3q-mCherry to LHA NT-HA neurons (Figure 1A).

To examine the response to activation of LHA NT cells, we injected the activating AAV-$hM3D_q$-mCherry bilaterally into the LHA of Nt^{cre} animals (Figure 1B) and, after at least 1 week of recovery, treated these Nt^{cre};LHA-hM3Dq-mCherry animals with vehicle or CNO (Figure 1, C and D). CNO treatment increased cFos-immunoreactivity (IR) in the LHA; this cFos-IR was mainly restricted to mCherry-IR neurons (Figure 1, C and D), consistent with the CNO-dependent activation of hM3Dq-mCherry-expressing LHA NT cells. CNO also increased cFOS-IR in the NAc, consistent with the notion that LHA NT neurons modulate the MLDA system (Figure 1, E and F).

We also treated Nt^{cre};LHA-hM3Dq-mCherry animals with vehicle or CNO in a metabolic chamber to determine the potential effect of LHA NT cell activation on locomotor activity and VO_2 (Figure 2, A–G). Pharmacogenetic activation of LHA NT cells nearly doubled ambulatory activity, and increased Z-axis activity by 8-fold during the 3 hours after CNO. Activation of LHA NT cells also increased VO_2 and VCO_2, consistent with the increased locomotor activity exhibited by these animals. Thus, the activation of LHA NT cells promotes locomotor activity in vivo.

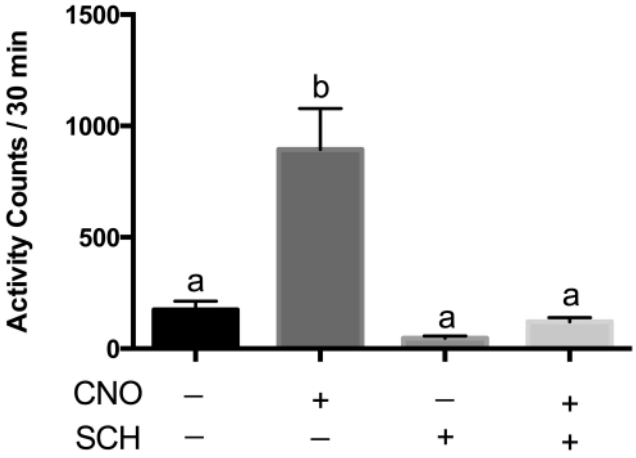

Figure 3. Blockade of ambulatory activity induced by hM3Dq-mediated activation of LHA NT neurons is blocked by peripheral administration of a D1R antagonist. Nt^{cre};LHA-hM3Dq-mCherry mice were acclimated to an open field area for 2 hours during the light cycle, after which time, their activity was monitored for 30 minutes after vehicle or CNO (0.3 mg/kg, ip) administration. Additional animals were pretreated with an ip injection (0.1 mg/kg) of the D1R antagonist, SCH23390 (SCH), 30 minutes before CNO administration. Activity (counts per min) is binned for the 30 minutes after vehicle (+/− SCH) and averaged per 30 minutes for CNO treatment (+/− SCH). All data are plotted as mean ± SEM, n = 7–8. Significance was determined by repeated measures ANOVA followed by Bonferroni post hoc analysis. Different letters indicate significant differences ($P \leq .001$); all other comparisons $P > .05$.

We have previously shown that, outside of the LHA, synaptic terminals from LHA NT cells primarily target midbrain regions, including the VTA (13). Because NT can enhance the activity of VTA DA cells (4, 25) and the release of VTA-derived DA into the striatum promotes locomotor activity (26), and we observed increased cFOS-IR in the NAc after activation of LHA NT cells, we examined the potential role for DA in the locomotor activity that accompanies the hM3Dq-mediated activation of LHA NT cells (Figure 3). Systemic administration of the D1R antagonist, SCH23390, did not significantly reduce baseline locomotor activity of animals in activity chambers but blunted the hM3Dq-mediated increase in activity to baseline levels. Thus, the activation of LHA NT cells promotes DA-dependent locomotor activity, suggesting that activation of LHA NT neurons promotes DA release in the NAc.

To assess this possibility, we performed in vivo microdialysis to examine the release of DA and its metabolites in the NAc of mice after the pharmacogenetic activation of LHA NT neurons in Nt^{cre};LHA-hM3Dq-mCherry animals (Figure 4 and Supplemental Figure 1). Locomotor activity was acutely increased by the injection of vehicle,

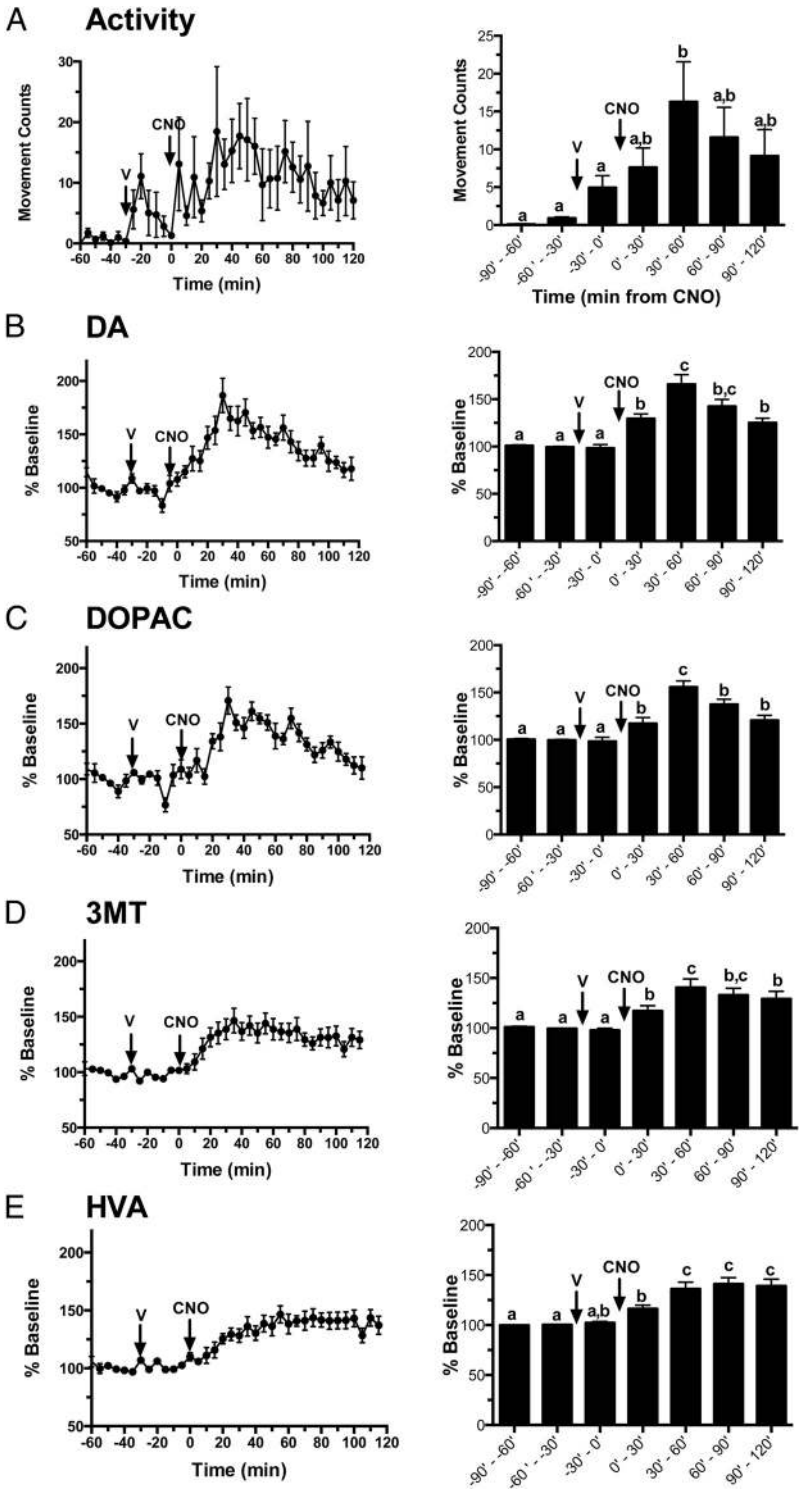

Figure 4. Extracellular DA and metabolites in NAc of *Nt*^{cre};LHA-hM3Dq-mCherry mice. Bilateral microdialysis probes were implanted into the NAc to monitor the effect of hM3Dq-mediated activation of LHA NT neurons. Vehicle was administered at t = −30 minutes, followed by CNO (0.3 mg/kg, ip, at t = 0 min) (arrows). Locomotor behavior from quantification of video (A) during microdialysis. Dialysate was assessed for (B) DA, (C) DOPAC, (D) 3MT, and (E) HVA. Locomotor behavior is shown as movement counts ± SEM. All in vivo microdialysis data are expressed as percent baseline ± SEM; n = 6–8. Left panels show data in 5-minute bins; right panels show 30-minute bins. Significance was determined by one-way ANOVA followed by Bonferroni post hoc analysis. Different letters indicate significant differences ($P \leq .05$).

although activity returned to baseline before the injection of CNO, which promoted a larger and sustained increase in locomotor activity (Figure 4A, consistent with Figures 2 and 3). Although neither the extracellular concentration of DA nor its metabolites (3,4-dihydroxyphenylacetic acid (DOPAC), 3-methyl tyrosine (3MT), and HVA) were altered by the injection of vehicle, CNO doubled the extracellular concentration of DA, which (like locomotor activity) peaked 30 minutes after CNO injection and remained elevated for at least the next 90 minutes. CNO also significantly increased the extracellular concentrations of DOPAC, 3MT, and HVA; the peaks of 3MT and HVA were prolonged relative to DA and DOPAC, consistent with the requirement for the cellular uptake of DA or DOPAC for the production of 3MT and HVA by intracellular monoamine oxidase. The increase in these metabolites also supports the notion that the increased extracellular DA observed reflects enhanced release rather than decreased DA reuptake. Thus, the activation of LHA NT neurons promotes NAc DA efflux, consistent with the DA dependence of the enhanced locomotor activity exhibited by mice after the activation of LHA NT cells.

Our finding that LHA NT cells project to the VTA, but not the NAc (13), suggests that neurotransmitters released by LHA NT neurons into the VTA act on DA neurons to promote the release of DA in the NAc. Because NT can postsynaptically increase N-methyl-D-aspartate-dependent Glu signaling in VTA DA neurons (4), we implanted microdialysis cannulae in the VTA of *Nt*^{cre};LHA-hM3Dq-mCherry animals and measured the extracellular concentration of NT (as well as GABA and Glu) in the VTA at baseline, after vehicle treatment, and after CNO administration (Figure 5).

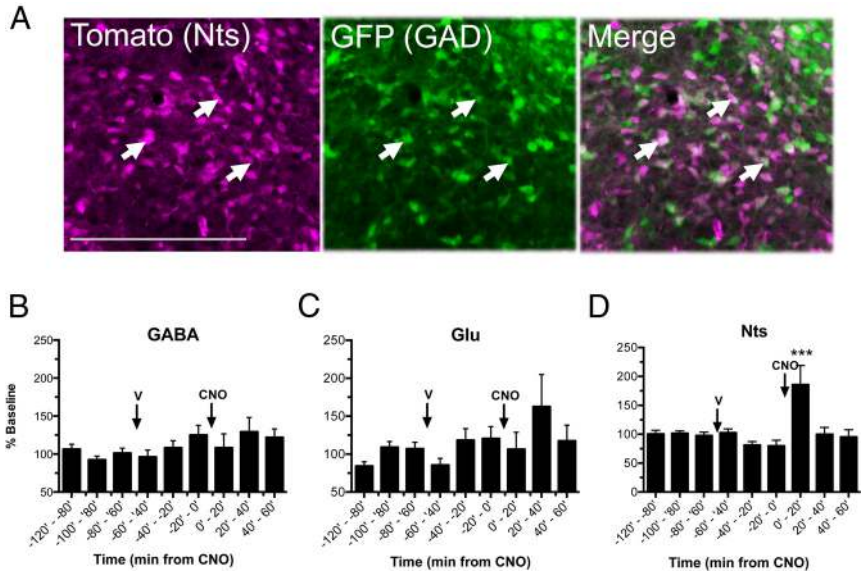

Figure 5. Neurotransmitter content and release by LHA NT neurons. Nt^{cre} mice were bred to the *ROSA26-tdTomato* and Gad1-GFP backgrounds to generate animals expressing *tdTomato* in in NT neurons and GFP in Gad1 cells. A, Representative images showing tdTomato-IR (NT; purple, left), GFP-IR (Gad1; green, middle) and merged (right) channels in the LHA of Nt^{cre} tdTomato; GAD1-GFP mice. Arrowheads indicate examples of colocalization. B–D, Extracellular concentrations of (B) GABA, (C) Glu, and (D) NT in the VTA of Nt^{cre};LHA-hM3Dq-mCherry mice. Vehicle (t = −60 min) and CNO (0.3 mg/kg, ip; t = 0 min) were administered systemically. In vivo microdialysis data are expressed as percent baseline ± SEM; n = 6. Significance was determined by one-way ANOVA followed by Bonferroni post hoc analysis; ***, $P \leq .001$ vs other times.

Although LHA NT neurons express *Gad1* (a marker of GABA neurons) (Figure 5A), CNO did not detectably increase the extracellular concentrations of GABA or Glu in the VTA (Figure 5, B and C). In contrast, however, the extracellular concentration of NT increased by almost 2-fold during the 20 minutes after CNO treatment (Figure 5D), demonstrating that the activation of LHA NT neurons promotes NT efflux into the VTA. Importantly, VTA NT concentrations return to baseline within 20 minutes of stimulation, suggesting that CNO-mediated activation of LHA NT cells promotes acute (rather than prolonged) VTA NT release.

To directly examine the possibility that LHA NT neurons may promote NAc DA efflux by acutely releasing NT into the VTA, we implanted VTA injection cannulae along with NAc microdialysis cannulae in Nt^{cre};LHA-hM3Dq-mCherry animals to examine extracellular DA in the NAc in the presence of VTA-applied SR14298A (an antagonist of NT1 receptors) (Figure 6 and Supplemental Figure 1). Although the application of SR14298A into the VTA did not alter NAc DA concentrations in the absence of CNO treatment, it abrogated the ability of activated LHA NT cells to promote NAc DA efflux. Thus, the acute release of NT into the VTA by LHA NT neurons promotes prolonged NAc DA efflux.

Discussion

Our present results reveal that LHA NT neurons stimulate NAc DA release to promote motivated behaviors such as ambulatory activity, thus revealing an important function for these cells. Additionally, we have mapped the circuits and mechanisms by which LHA NT neurons mediate this effect: LHA NT neurons project to the VTA, where they promote acute NT release; NT acts on NTR1 in the VTA to promote prolonged NAc DA release (Figure 6C).

In addition to the use of genetic (eg, Nt^{cre}, AAV-hM3Dq-mCherry) and pharmacologic techniques, this analysis required the fabrication and use of microdialysis probes small enough to permit the neuroanatomically precise sampling of extracellular fluid in the mouse NAc and VTA, as well as the development of techniques to quantitatively measure NT at physiologic concentrations in the resultant samples. To our knowledge, this represents the first report to measure changes in neuropeptide release in the intact mouse; this technique enabled us to directly assess the timing and amplitude of intra-VTA NT release induced by pharmacogenetic activation of LHA NT neurons. The requirement that we collect sufficient sample volume to permit NT detection by subsequent MS analysis dictates a prolonged (20 min) sampling time, thus limiting temporal resolution. Even so, it is clear that DREADD-mediated activation of LHA NT neurons promotes acute NT release and also that VTA NT concentrations return to baseline by 20 minutes after stimulation.

In contrast to the rapid rise and fall of VTA NT concentrations, the hM3Dq-promoted increase in NAc DA concentration (which requires VTA NT signaling) continues for at least 2 hours, much longer than the increase in VTA NT. These findings suggest that VTA NT promotes a durable increase in NAc DA release (and accompanying locomotor behavior) that continues long after VTA NT has returned to baseline and that the action of LHA NT cells mediates the long-term rather than acute modulation of the MLDA system. Consistent with this long-term activation, Kempadoo et al (4) showed that NTR1 antagonism blocks the increase postsynaptic NDMA response of VTA DA neurons to the optogenetic activation of

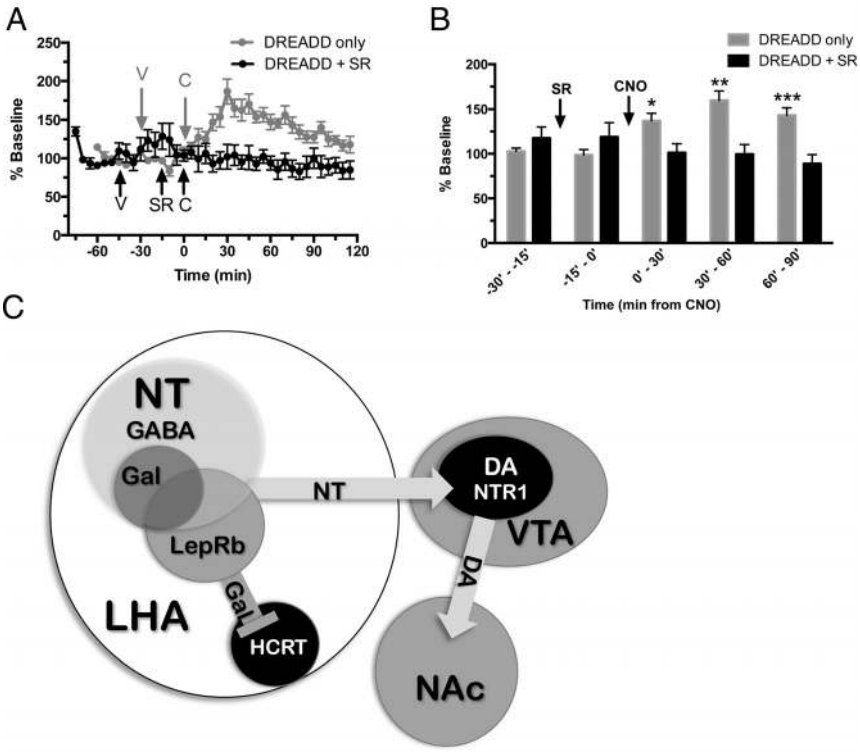

Figure 6. Effect of NT1R antagonism on LHA NT-DREADD-evoked NAc DA release. Unilateral microdialysis probes were implanted into the NAc with ipsilateral cannulation of the VTA. Vehicle, NtsR1-antagonist SR142948A (SR; dose via intra-VTA injection) and CNO (0.3 mg/kg, ip; t = 0 min) were administered at the indicated times. A, Extracellular DA concentrations in the NAc. B, Data from A plotted in 15- or 30-minute bins. Data are expressed as percent baseline ± SEM; n = 6. Significance was determined by one-way ANOVA followed by Bonferroni post hoc analysis. *, $P < .1$; **, $P < .01$; ***, $P < .001$. C, Model of the control of the MLDA system via LHA NT neurons. LHA NT neurons contain the neurotransmitter GABA. Some of these NT neurons express the LepRb and locally regulate HCRT neuronal function, via the neuropeptide Gal. A potentially separate population of LHA NT neurons may directly project to the VTA and release NT onto NTR1-expressing DA neurons to regulate the MLDA system through projections to the NAc. Note that although the figure is simplified for easier viewing, it is possible that interneurons could lie between LHA NT neurons and OX or DA neurons.

LHA→VTA fibers. That LHA NT neurons should mediate lasting effects on MLDA function makes teleological sense, because many LHA NT cells respond directly to leptin (13), which reflects long-term energy stores and mediates largely chronic (rather than acute) effects on neural systems (27).

Although we have recently demonstrated that the hM3Dq-mediated activation of LHA NT neurons also inhibits LHA HCRT neurons (14), the mechanism for this effect is distinct from that by which LHA NT neurons promote NAc DA efflux. Not only do the neural connections by which these responses occur differ (intra-LHA vs LHA→VTA projections) but also NT (which is required for increased NAc DA efflux) is not responsible for controlling the activity of HCRT cells. Rather, the inhibitory neuropeptide, galanin (Gal), which is found in some LHA NT neurons, inhibits the firing of HCRT cells (14). Thus, LHA NT neurons mediate their effects on HCRT cells and the MLDA via distinct neurotransmitters. We do not know whether these distinct mechanisms of LHA NT neuron action reflect different patterns of neurotransmitter release by these cells in the LHA and VTA, or merely the innate responsiveness of HCRT and VTA neurons to the different neuropeptides.

Interestingly, although LHA NT neurons display markers of gamma amino butyric acid (GABA) production and release (*Gad1* and *Slc32a1*), we did not detect VTA GABA release upon activation of these neurons. Although it is possible that the long collection times for VTA microdialysis samples (which are required for NT detection) could fail to detect a transient increase in VTA GABA after the activation of LHA NT cells, this technique readily detects prolonged release of DA and its metabolites downstream in the NAc. We were also unable to detect a role for GABA in the acute inhibition of HCRT neurons by LHA NT cells (14). Thus although LHA NT neurons are genetically GABAergic, GABA release by these cells may play less important roles than their neuropeptide transmitters.

Because LHA NT neurons respond to a variety of physiologic signals (such as leptin, dehydration, and inflammation), this LHA NT→VTA NtsR1→NAc DA circuit that we have mapped may link these stimuli to the long-term modulation of VTA DA neurons, NAc DA efflux, and thus locomotor activity and other DA-dependent behaviors. Indeed, disruption of LepRb in LHA NT cells diminishes locomotor activity and measures of MLDA function (13), suggesting that leptin action on LHA NT cells may control MLDA function by modulating NT release in the VTA. Additional work will be required to understand the contribution of NT signaling to the control of MLDA function by the various stimuli that modulate the activity of LHA NT neurons.

Acknowledgments

Address all correspondence and requests for reprints to: Robert T. Kennedy, PhD, Department of Chemistry, University of Michigan,

Ann Arbor, MI 48109-1055. E-mail: rtkenn@umich.edu; or Martin G. Myers, Jr, MD, PhD, Division of Metabolism, Endocrinology and Diabetes, Department of Internal Medicine, University of Michigan Medical School, 6317 Brehm Tower, 1000 Wall Street, Ann Arbor, MI 48105-1055. E-mail: mgmyers@umich.edu.

Present address for G.M.L.: Department of Physiology, Michigan State University. Lansing, MI 48824.

This work was supported by National Institutes of Health Grants DK078056 (to M.G.M.), EB003320 (to R.T.K.), DK090101 (to G.M.L.), and HL007853 (to C.M.P.); the American Diabetes Association (M.G.M.); the American Heart Association (M.G.M.); and the Marilyn H. Vincent Foundation (M.G.M.).

Disclosure Summary: The authors have nothing to disclose.

References

1. **Hyman SE, Malenka RC, Nestler EJ.** Neural mechanisms of addiction: the role of reward-related learning and memory. *Annu Rev Neurosci*. 2006;29:565–598.
2. **Berthoud HR.** Interactions between the "cognitive" and "metabolic" brain in the control of food intake. *Physiol Behav*. 2007; 91:486–498.
3. **Shizgal P, Fulton S, Woodside B.** Brain reward circuitry and the regulation of energy balance. *Int J ObesRelat Metab Disord*. 2001; 25(suppl 5):S17–S21.
4. **Kempadoo KA, Tourino C, Cho SL, et al.** Hypothalamic neurotensin projections promote reward by enhancing glutamate transmission in the VTA. *J Neurosci*. 2013;33(18):7618–7626.
5. **Sakurai T, Amemiya A, Ishii M, et al.** Orexins and orexin receptors: a family of hypothalamic neuropeptides and G protein-coupled receptors that regulate feeding behavior. *Cell*. 1998;92(4):573–585.
6. **Boutrel B, Cannella N, de Lecea L.** The role of hypocretin in driving arousal and goal-oriented behaviors. *Brain Res*. 2010;1314:103–111.
7. **Georgescu D, Sears RM, Hommel JD, et al.** The hypothalamic neuropeptide melanin-concentrating hormone acts in the nucleus accumbens to modulate feeding behavior and forced-swim performance. *J Neurosci*. 2005;25(11):2933–2940.
8. **Opland D, Sutton A, Woodworth H, et al.** Loss of neurotensin receptor-1 disrupts the control of the mesolimbic dopamine system by leptin and promotes hedonic feeding and obesity. *Mol Metab*. 2013; 2(4):423–434.
9. **Leonetti M, Brun P, Sotty F, et al.** The neurotensin receptor antagonist SR 142948A blocks the efflux of dopamine evoked in nucleus accumbens by neurotensin ejection into the ventral tegmental area. *Naunyn Schmiedebergs Arch Pharmacol*. 2002;365(6):427–433.
10. **Panayi F, Colussi-Mas J, Lambás-Señas L, Renaud B, Scarna H, Bérod A.** Endogenous neurotensin in the ventral tegmental area contributes to amphetamine behavioral sensitization. *Neuropsychopharmacology*. 2005;30(5):871–879.
11. **Luttinger D, King RA, Sheppard D, Strupp J, Nemeroff CB, Prange AJ Jr.** The effect of neurotensin on food consumption in the rat. *Eur J Pharmacol*. 1982;81(3):499–503.
12. **Sahu A, Carraway RE, Wang YP.** Evidence that neurotensin mediates the central effect of leptin on food intake in rat. *Brain Res*. 2001;888(2):343–347.
13. **Leinninger GM, Opland DM, Jo YH, et al.** Leptin action via neurotensin neurons controls orexin, the mesolimbic dopamine system and energy balance. *Cell Metab*. 2011;14(3):313–323.
14. **Goforth PB, Leinninger GM, Patterson CM, Satin LS, Myers MG, Jr.** Leptin acts via lateral hypothalamic area neurotensin neurons to inhibit orexin neurons by multiple GABA-independent mechanisms. *J Neurosci*. 2014;34(34):11405–11415.
15. **Abe H, Yanagawa Y, Kanbara K, et al.** Epithelial localization of green fluorescent protein-positive cells in epididymis of the GAD67-GFP knock-in mouse. *J Androl*. 2005;26(5):568–577.
16. **Sanz E, Yang L, Su T, Morris DR, McKnight GS, Amieux PS.** Cell-type-specific isolation of ribosome-associated mRNA from complex tissues. *Proc Natl Acad Sci USA*. 2009;106(33):13939–13944.
17. **Krashes MJ, Koda S, Ye C, et al.** Rapid, reversible activation of AgRP neurons drives feeding behavior in mice. *J Clin Invest*. 2011; 121(4):1424–1428.
18. **Armbruster BN, Li X, Pausch MH, Herlitze S, Roth BL.** Evolving the lock to fit the key to create a family of G protein-coupled receptors potently activated by an inert ligand. *Proc Natl Acad Sci USA*. 2007; 104(12):5163–5168.
19. **Mabrouk OS, Kennedy RT.** Simultaneous oxytocin and arg-vasopressin measurements in microdialysates using capillary liquid chromatography-mass spectrometry. *J Neurosci Methods*. 2012;209(1): 127–133.
20. **Mabrouk OS, Semaan DZ, Mikelman S, Gnegy ME, Kennedy RT.** Amphetamine stimulates movement through thalamocortical glutamate release. *J Neurochem*. 2014;128(1):152–161.
21. **Song P, Mabrouk OS, Hershey ND, Kennedy RT.** In vivo neurochemical monitoring using benzoyl chloride derivatization and liquid chromatography-mass spectrometry. *Anal Chem*. 2012;84(1): 412–419.
22. **Li Q, Zubieta JK, Kennedy RT.** Practical aspects of in vivo detection of neuropeptides by microdialysis coupled off-line to capillary LC with multistage MS. *Anal Chem*. 2009;81(6):2242–2250.
23. **Watts AG, Boyle CN.** The functional architecture of dehydration-anorexia. *Physiol Behav*. 2010;100(5):472–477.
24. **Grossberg AJ, Zhu X, Leinninger GM, et al.** Inflammation-induced lethargy is mediated by suppression of orexin neuron activity. *J Neurosci*. 2011;31(31):11376–11386.
25. **Stowe ZN, Nemeroff CB.** The electrophysiological actions of neurotensin in the central nervous system. *Life Sci*. 1991;49(14):987–1002.
26. **Nestler EJ.** Is there a common molecular pathway for addiction? *Nat Neurosci*. 2005;8(11):1445–1449.
27. **Myers MG Jr, Olson DP.** Central nervous system control of metabolism. *Nature*. 2012;491(7424):357–363.